J Mater Sci (2009) 44:1800–1812
DOI 10.1007/s10853-009-3274-5

Depth profile XPS analysis of polymeric materials by C_{60}^+ ion sputtering

Takuya Nobuta · Toshio Ogawa

Received: 4 November 2008 / Accepted: 13 January 2009 / Published online: 7 February 2009

Abstract When the depth profile of chemical composition is studied with X-ray photoelectron spectroscopy (XPS), the Ar^+ ion sputtering method is generally adopted. However, in the case of polymers, chemical composition is destroyed, and so it is impossible to obtain accurate depth profile on polymers. In this research, the depth profile XPS analysis of aliphatic polymers, aromatic polymers, fluorine containing polymers, and natural polymers were conducted with the sputtering source being C_{60}^+ ion, and the degree of damage was examined while comparing the results with the case of conventional Ar^+ ion. It was found that Ar^+ ion induces significant carbonization in all the polymers above-mentioned. Meanwhile, it turned out that C_{60}^+ ion causes little damage to most polymers. However, in the case of the non-aromatic polymers containing halogen, hydroxyl, carboxyl, and ether groups in their backbones, the following three damage modes were found: (1) the functional group ratio changes by over ±10%; (2) new functional groups are formed; (3) the above (1) and (2) phenomena occur simultaneously.

Introduction

X-ray photoelectron spectroscopy (XPS) is a method for analyzing the elemental composition and chemical-bonding state of materials including organic and inorganic substances on the solid sample surface. Especially, this method is excellent in the study of polymer materials, because it is possible to analyze the functional groups in the region around a depth of several nm, which cannot be observed by other methods. When the depth profile of chemical composition is studied, it is common to repeat sputtering and analysis using Ar^+ ion. However, when a polymer material is analyzed with the Ar^+ ion sputtering method, Ar^+ ion destroys its chemical structure, and so accurate information cannot be obtained in many cases [1, 2]. Therefore, the Ar^+ ion sputtering method is not appropriate for the depth profile analysis of polymer materials. Recently, it is attempted to use cluster ions, such as SF_5^+, Au_n^+, Bi_n^+, and C_{60}^+, as the primary ion source and the sputter source of Time of Flight Secondary Ion Mass Spectroscopy (TOF-SIMS), in order to reduce the damage due to ion sputtering and increase sputtering yield, and its application to surface analysis is paid to attention [3–13]. As an advantage of cluster ions, it is possible to reduce the damage to surface, because the energy of collision between the sample surface and an atom that constitutes a cluster ion is low. In addition, the atoms constituting a primary ion simultaneously collide with the extremely shallow region of the sample surface, and so irradiation energy density increases, and then the increase in the emission intensity of a secondary ion can be expected. Furthermore, the research utilizing the simulation of molecular dynamics shows the sputtering mechanism with Ga^+ ion or C_{60}^+ ion [14, 15]. In the case of the single-atom Ga^+ ion, it reaches the inside of the sample in the almost vertical direction, and then diffuses cylindrically in the energy propagation region. Accordingly, it is considered that mixing occurs in the region where ions can reach, and then thickness of the mixing layer reaches the detectable depth with XPS. On the other hand, C_{60}^+ ion, which is a

---

T. Nobuta (✉)
Nitto Analytical Techno-Center Co., Ltd., 1-1-2, Shimohozumi, Ibaraki, Osaka 567-8680, Japan
e-mail: takuya-nobuta@gg.nitto.co.jp

T. Ogawa
Laboratory for Ecological Polymer Chemistry, Kanazawa Institute of Technology, 7-1, Ohgigaoka, Nonoichi, Ishikawa 921-8501, Japan

cage-like molecule with a diameter of about 0.7 nm, collapses upon colliding with the sample surface, and so it is considered that energy is dispersed in random directions and it does not reach the inside of the sample. The thickness of the mixing layer produced by $C_{60}{}^{+}$ ion is ignorable in the XPS analysis. In addition, the optimum conditions for the $C_{60}{}^{+}$ ion gun were discussed. Gillen et al. reported that in the case where $C_{60}{}^{+}$ ion is irradiated on the Si substrate with an accelerating voltage of 3.0–14.5 keV, Si undergoes sputtering when accelerating voltage is 14.5 keV, and carbon accumulates on the Si substrate surface when accelerating voltage is less than 9 keV [16]. Miyayama et al. reported that in the case where the incidence angle of $C_{60}{}^{+}$ ion is changed in the range from 0 to 75 degrees, sputtering yield is higher as the angle is larger, and it is possible to conduct analysis without damaging polymers significantly or inducing carbon accumulation [17]. These research reports indicate the possibility of utilizing $C_{60}{}^{+}$ ion for the depth profile XPS analysis. There have been some reports on the $C_{60}{}^{+}$ ion sputtering-based XPS analysis, which was applied to PTFE [18] and the depth profile analysis of ArF immersion resists [19]. However, there have been no reports regarding the materials other than the above-mentioned ones, and the degree of damage to each polymer due to $C_{60}{}^{+}$ ion sputtering has not been discussed yet, and so it is still impossible to check whether or not this method is practical. We conducted the depth profile XPS analysis of aliphatic polymers, aromatic polymers, fluorine containing polymers, and natural polymers with the $C_{60}{}^{+}$ ion sputtering. The ratio of change of each functional groups derived from the chemical structure of each polymer was compared with that of the Ar^{+} ion sputtering.

Experimental

Materials

Examined aliphatic, aromatic, fluorine containing, and natural polymers are shown in Table 1.

XPS equipment and analysis

As an XPS device, the authors used PHI Quantera SXM equipped with the Ar^{+} ion and $C_{60}{}^{+}$ ion guns (PHI 06-C60) [20]. As the $C_{60}{}^{+}$ ion sputtering conditions, the authors set accelerating voltage 10 kV, sample current 10 nA, sputtering area 0.5 mm × 2.0 mm, and incidence angle 70 degrees from the direction vertical to the sample surface. For the analysis, the Al-Kα characteristic X-ray ($h\nu = 1486.6$ eV) was adopted, and accelerating voltage and irradiation power were set to be 15 kV and 25 W, respectively. The XPS analysis was carried out while conducting charge neutralization under the ultrahigh vacuum condition (below 10^{-7} Pa), after setting the measurement range to about 100 μm and photoelectron take-off angle 45 degrees with respect to the sample surface. The $C_{60}{}^{+}$ ion sputtering was conducted at 1-min intervals, from the surface to the depth of 100 nm. The C1s XPS spectra observed at 1-min intervals were divided at the peaks induced by functional groups, and their ratios were calculated. In addition, several kinds of polymers were studied with the conventional Ar^{+} ion sputtering method (accelerating voltage: 1 kV) in the same way, and the results were compared with those for $C_{60}{}^{+}$ ion. Here, the authors divided spectra based on peaks and identified functional groups with reference to a handbook [21]. For the measurement of the sputtering depth of each material, the authors placed metal mesh on the sample surface, and adopted the mesh-replica method [22], in which the mesh pattern after sputtering is scanned with a stylus profilometer.

The lattice-like metal mesh was placed on the sample surface, which was then wrapped with aluminum foil. The metal mesh and aluminum foil were removed after sputtering. The sputtering rate for each material was determined comparing the sputtered and non-sputtered area by means of the stylus profilometer. After sputtering with Ar^{+} ion, the sputtering rate in PVA and PC was 5 nm min^{-1}; in ETFE and TAC, 10 nm min^{-1}. In the case of $C_{60}{}^{+}$ ion, the sputtering rate in PVA was 10 nm min^{-1}; in PET, 5 nm min^{-1}; in ETFE and TAC, 20 nm min^{-1}.

Results and discussion

Ar^{+} ion sputtering method

The depth profiles of several kinds of polymers were analyzed with the conventional Ar^{+} ion sputtering method. Figure 1 shows the (a) C1s XPS spectra and (b) XPS depth profile of PGA, which is an aliphatic polymer. The C1s XPS spectra after sputtering (50 and 100 nm) differs from that before the sputtering. The peak intensities of the C–O and COO bonds derived from the PGA structure were extremely low. In (b) XPS depth profile, when sputtering was repeated, the ratios of the C–O bond and the COO bond gradually decreased, and after the 100 nm sputtering, each functional group decreased by about 40%. Table 2 shows the rate of change of each functional group of other aliphatic polymers after the Ar^{+} ion sputtering to a depth of 100 nm. It was found that in either of the PLA, PAA, PVA, PEG, and PVC, the ratio of the oxygen containing functional groups derived from each structure decreases by over 20%. In addition, with regard to PVA, the emergence of a new functional group that can be identified as the C=O bond was surprisingly observed. The (a) C1s XPS spectra and (b) XPS depth profile of this PVA are shown in Fig. 2.

Table 1 Polymers used for the experiment

Classification	Polymers[a]	Abbreviation
Aliphatic polymers	Poly(glycolic acid)	PGA
	Poly(lactic acid)	PLA
	Poly[oxy(1-oxohexane-1,6-diyl)]	PCL
	Poly(1,4-butylene succinate)	PBS
	Poly(acrylicacid)	PAA
	Poly(methyl methacrylate)	PMMA
	Poly(oxymethylene-co-oxyethylene)	POM
	Poly(vinyl alcohol)	PVA
	Poly(ethylene/1-hydroxyethylene)	EVOH
	Poly(ethylene glycol)	PEG
	Poly(vinyl chloride)	PVC
	Poly(1,1-dichloro ethylene)	PVDC
	Poly[imino(1-oxohexane-1,6-diyl)]	PA
	Poly(acrylonitrile)	PAN
Aromatic polymers	Poly[oxycarbonyloxy-1,4-phenylene (dimethylmethylene)-1,4-phenylene]	PC
	Poly(ethylene terephthalate)	PET
	Poly(oxybutane-1,4-diyloxyterephthaloyl)	PBT
	Poly(ethylene2,6-naphthalene dicarboxylate)	PEN
	Poly(oxy-1,4-phenyleneoxy-1,4-phenylene carbonyl-1,4-phenylene)	PEEK
	Poly(amideimide)	PAI
	Poly[2,2'-(m-phenylene)-5,5'-bibenzimidazole]	PBI
	Poly(oxybutane-1,4-diyloxycarbonylimino-1,4-phenylenemethylene-1,4-phenyleneiminocarbonyl)	PU
	Poly[oxy-1,4-phenylenesulfonyl-1,4-phenyleneoxy-1,4-phenylene(dimethylmethylene)-1,4-phenylene]	PSF
	Poly(oxy-1,4-phenylenesulfonyl-1,4-phenylene)	PES
Fluorine containing polymers	Poly(ethylene/1,1,2,2-tetrafluoroethylene)	PTFE
	Poly(1,1-difluoroethylene)	PVDF
	Poly(difluoromethylene)	ETFE
	Poly(tetrafluoroethylene-co-perfluorovinylether)	PFA
Natural polymers	Poly({3,4-bis(acetyloxy)-6-[(acetyloxy)methyl]tetrahydro-2H-pyran-2,5-diyl}oxy)	TAC
	Poly{[3,4-dihydroxy-6-(hydroxymethyl)tetrahydropyran-2,5-diyl]oxy}	CEL

[a] The IUPAC name of polymers quoted the database http://polymer.nims.go.jp/

Figure 3 shows the (a) C1s XPS spectra and (b) XPS depth profile of PC, which is an aromatic polymer. The C1s XPS spectra after sputtering (50 and 100 nm) also differs from that before sputtering. The peaks of the C–O, O–COO bonds, and π–π* derived from the PC structure disappeared. In (b) XPS depth profile, oxygen containing functional groups and π–π* were not detected at all in the depth of 10 nm. The analytical result of other aromatic polymers is shown in Table 2. These results reveal that oxygen containing functional groups and π–π* are hardly detected and carbonization occurs considerably after the Ar^+ ion sputtering in these polymers.

Figure 4 shows the (a) C1s XPS spectra and (b) XPS depth profile of PTFE, which is a fluorine containing polymer. The C1s XPS spectra, after sputtering (50 and 100 nm) showed new peaks that can be identified as the C–CF_2, CF, and CF_3 bonds in addition to the original CF_2 bond. In (b) XPS depth profile, as sputtering was repeated, the ratios of the C–CF_2 bond, the CF bond, and the CF_3 bond increased, and the original CF_2 bond decreased by 40%. Table 2 also shows the results of the study on PVDF and ETFE. It was found that sputtering induces the formation of new bonds other than the original ones, changing their chemical structures, like the case of PTFE.

Figure 5 shows the (a) C1s XPS spectra and (b) XPS depth profile of TAC, which is a natural polymer. The C1s XPS spectra after sputtering (50 and 100 nm) differs from that before sputtering. The peak intensities of the C–O,

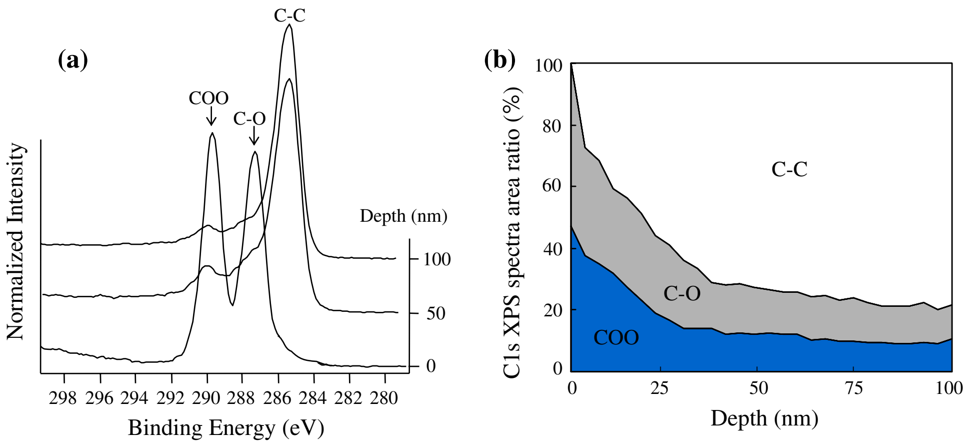

Fig. 1 **a** C1s XPS spectra of PGA, which were obtained before sputtering and after 50 and 100 nm sputtering. **b** XPS depth profile of PGA obtained using Ar^+ ion sputtering. The depth profile of C–C, C–O, and COO bonds were obtained by analyzing C1s XPS spectra of every 1-min sputtering. The sputtering depth means reduced value of PVA (5 nm min^{-1})

O–C–O, and COO bonds derived from the TAC structure were extremely low. In (b) XPS depth profile, as sputtering was repeated, the ratio of oxygen containing functional groups decreased gradually.

In the depth profile analysis based on the Ar^+ ion sputtering, all of the analyzed polymers showed some changes in their chemical structures, such as surface carbonization and the formation of new functional groups. Such changes in chemical structure are considered due to the bond dissociation, compositional mixing, and recombination by Ar^+ ion sputtering.

$C_{60}{}^+$ ion sputtering method

Aliphatic polymers

Figure 6 shows the (a) C1s XPS spectra and (b) XPS depth profile of PGA. In the case of $C_{60}{}^+$ ion sputtering, the spectra of (a) C1s XPS spectra did not change through sputtering, and there were no changes in the peak intensities of these bonds. With regard to (b) XPS depth profile, the ratio of change of oxygen containing functional groups after the 100-nm sputtering was less than ±2%. That is, we could analyze the polymer without causing little damage to it. Table 3 shows the ratio of change of each functional groups of other aliphatic polymers after the $C_{60}{}^+$ ion sputtering at a depth of 100 nm. This table reveals that with regard to the biodegradable polymers PLA, PCL, and PBS, the nitrogen containing polymers PA and PAN, and PMMA, the ratio of change of the functional group derived from each chemical structure is less than ±5%, and the damage due to $C_{60}{}^+$ ion is extremely small. It was concluded that the $C_{60}{}^+$ ion sputtering can be practically applied to the depth profile XPS analysis of the above-mentioned polymers. On the other hand, there are some aliphatic polymers that are damaged by $C_{60}{}^+$ ion sputtering; in the case of PAA, POM, PEG, PVC, and PVDC, the ratio of the functional group derived from each structure changed by over ±10%. In addition, in the case of PVA, the new peak that can be identified as the C=O bond was observed after sputtering. The (a) C1s XPS spectra and (b) XPS depth profile of this PVA are shown in Fig. 7. In (a) C1s XPS spectra, a new peak that can be identified as the C=O bond was detected in after sputtering (50 and 100 nm). In (b) XPS depth profile, through the appearance of the C=O bond, suggests that hydroxyl group is oxidized because the ratio of the C–C bond did not change, and the ratio of the C–O bond decreased. In the case of EVOH, the appearance of the C=O bond was observed like the PVA case, and so it is considered that the hydroxyl group included in the EVOH structure is oxidized. These results reveal that the aliphatic polymers having ester bond in their backbones are hardly damaged by $C_{60}{}^+$ ion sputtering, but the aliphatic polymers having halogen group, hydroxyl group, carboxyl group, and ether bond in their backbones suffer damage. Nevertheless, the degree of damage to each polymer due to $C_{60}{}^+$ ion sputtering is much lower than that due to Ar^+ ion sputtering.

Aromatic polymers

Figure 8 shows the (a) C1s XPS spectra and (b) XPS depth profile of PC. The spectra form of after sputtering (50 and 100 nm) did not change through sputtering, and there were no changes in the peak intensities of these bonds. With regard to (b) XPS depth profile, the ratios of change of the C–O, O–COO bonds, and π–π^* through the 100-nm sputtering were less than ±2%. That is, we could analyze the polymer without causing little damage to it. Table 4 shows the ratio of change of each functional group of other aromatic polymers after the $C_{60}{}^+$ ion sputtering at a depth of

Table 2 Change of the functional group content before and after Ar$^+$ ion sputtering in various polymers

	Abbreviation	Chemical constitution	Functional group	C1s XPS spectra area ratio (%)		Difference (%)
				Before sputtering	After sputtering[a]	
Aliphatic polymers	PGA	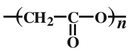 $\left(CH_2-\underset{\underset{O}{\Vert}}{C}-O \right)_n$	C–C[b]	0	77	+77
			C–O	51	11	−40
			COO	49	12	−37
	PLA	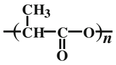 $\left(\overset{\overset{CH_3}{\vert}}{CH}-\underset{\underset{O}{\Vert}}{C}-O \right)_n$	C–C	38	80	+42
			C–O	31	11	−20
			COO	31	9	−22
	PAA	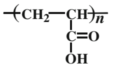 $\left(CH_2-\underset{\underset{\underset{OH}{\vert}}{C=O}}{\underset{\vert}{CH}} \right)_n$	C–C	70	91	+21
			COO	30	9	−21
	PVA	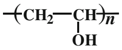 $\left(CH_2-\underset{\underset{OH}{\vert}}{CH} \right)_n$	C–C	49	77	+28
			C–O	51	19	−32
			C=O[b]	0	4	+4
	PEG	$\left(CH_2-CH_2-O \right)_n$	C–C	0	61	+61
			C–O	100	39	−61
	PVC	$\left(CHCl-CH_2 \right)_n$	C–C	57	80	+23
			C–Cl	43	20	−23
Aromatic polymers	PC	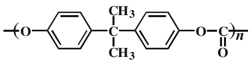	C–C	74	100	+26
			C–O	16	0	−16
			O–COO	6	0	−6
			π–π*	4	0	−4
	PET	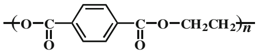	C–C	57	97	+40
			C–O	20	0	−20
			COO	19	3	−16
			π–π*	4	0	−4
	PEN	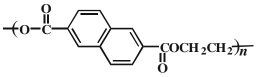	C–C	66	98	+32
			C–O	16	0	−16
			COO	14	2	−12
			π–π*	4	0	−4
	PSF	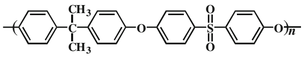	C–C, C–S	81	99	+18
			C–O	14	0	−14
			π–π*	5	1	−4
Fluorine containing polymers	PTFE	$\left(CF_2-CF_2 \right)_n$	C–CF$_2$[b]	0	10	+10
			CF[b]	0	18	+18
			CF$_2$	100	60	−40
			CF$_3$[b]	0	12	+12
	PVDF	$\left(CF_2-CH_2 \right)_n$	C–CF$_2$	52	69	+17
			CF[b]	0	24	+24
			CF$_2$	48	7	−41
	ETFE	$\left(CF_2-CF_2 \right)_n \left(CH_2-CH_2 \right)_m$	C–C	36	59	+23
			CF[b]	0	22	+22
			CF$_2$	64	15	−49
			CF$_3$[b]	0	4	+4

Table 2 continued

	Abbreviation	Chemical constitution	Functional group	C1s XPS spectra area ratio (%) Before sputtering	C1s XPS spectra area ratio (%) After sputtering[a]	Difference (%)
Natural polymer	TAC	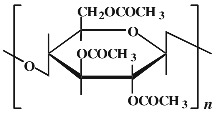	C–C	32	74	+42
			C–O	35	15	−20
			O–C–O	7	3	−4
			COO	26	8	−18

[a] Value in 100 nm depth

[b] Functional group newly detected after sputtering

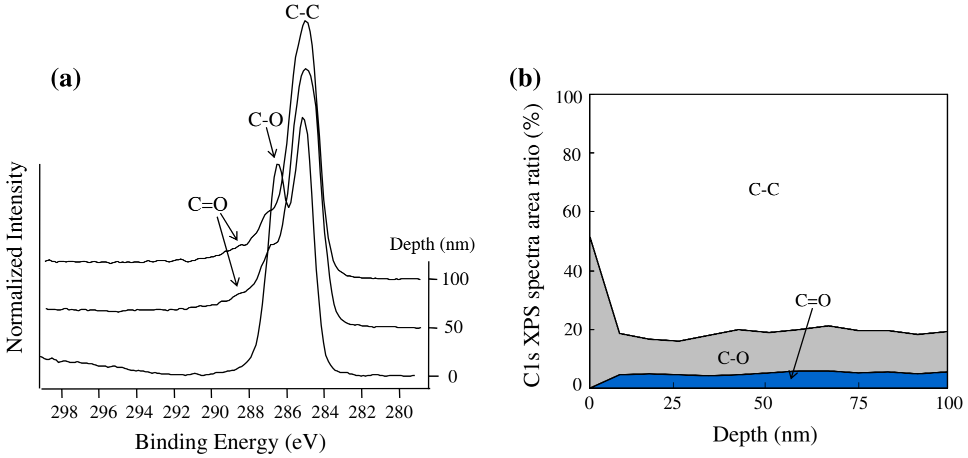

Fig. 2 **a** C1s XPS spectra of PVA, which were obtained before sputtering and after 50 and 100 nm sputtering. **b** XPS depth profile of PGA obtained using Ar$^+$ ion sputtering. The depth profile of C–C, C–O, and C=O bonds were obtained by analyzing C1s XPS spectra of every 1-min sputtering. The sputtering depth means reduced value of PVA (5 nm min^{-1})

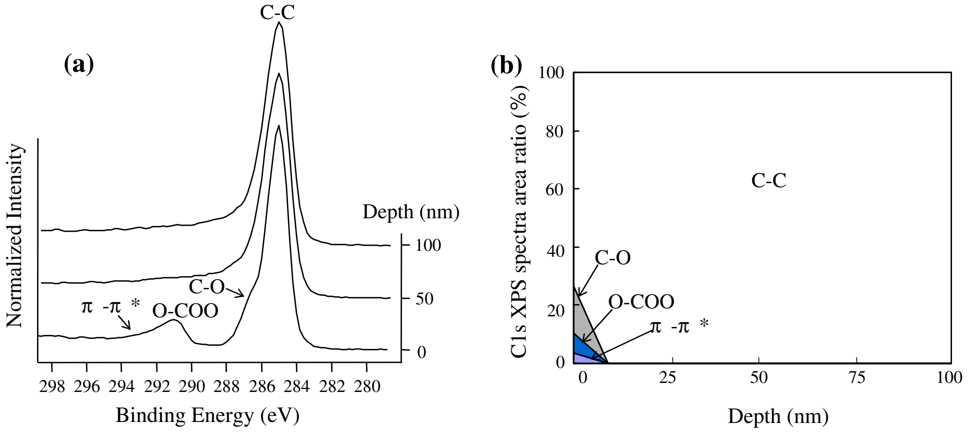

Fig. 3 **a** C1s XPS spectra of PC, which were obtained before sputtering and after 50 and 100 nm sputtering. **b** XPS depth profile of PC obtained using Ar$^+$ ion sputtering. The depth profile of C–C, C–O, O–COO bonds, and π–π* were obtained by analyzing C1s XPS spectra of every 1-min sputtering. The sputtering depth means reduced value of PC (5 nm min^{-1})

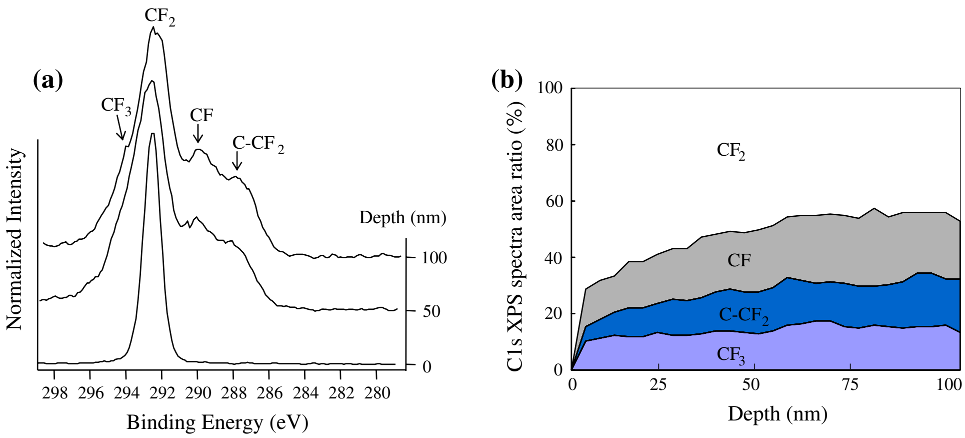

Fig. 4 a C1s XPS spectra of PTFE, which were obtained before sputtering and after 50 and 100 nm sputtering. **b** XPS depth profile of PTFE obtained using Ar^+ ion sputtering. The depth profile of CF_2, CF, C–CF_2, and CF_3 bonds were obtained by analyzing C1s XPS spectra of every 1-min sputtering. The sputtering depth means reduced value of ETFE (10 nm min^{-1})

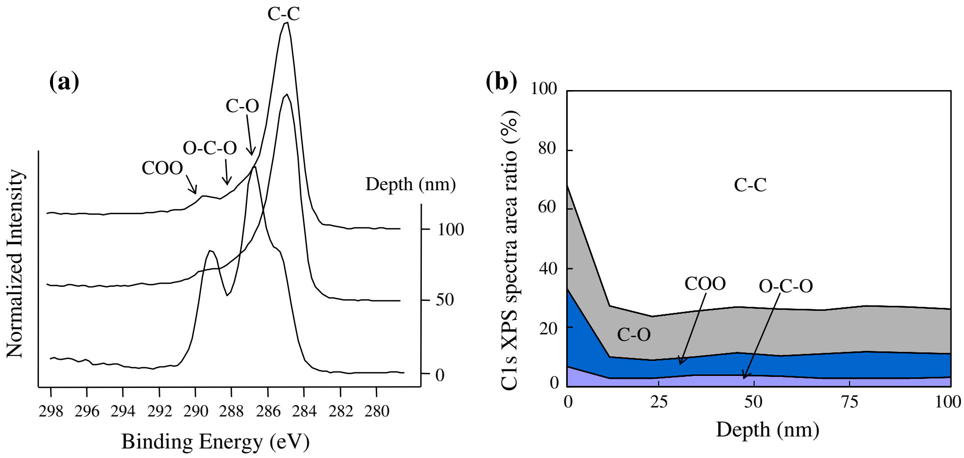

Fig. 5 a C1s XPS spectra of TAC, which were obtained before sputtering and after 50 and 100 nm sputtering. **b** XPS depth profile of TAC obtained using Ar^+ ion sputtering. The depth profile of C–C, C–O, O–C–O, and COO bonds were obtained by analyzing C1s XPS spectra of every 1-min sputtering. The sputtering depth means reduced value of TAC (10 nm min^{-1})

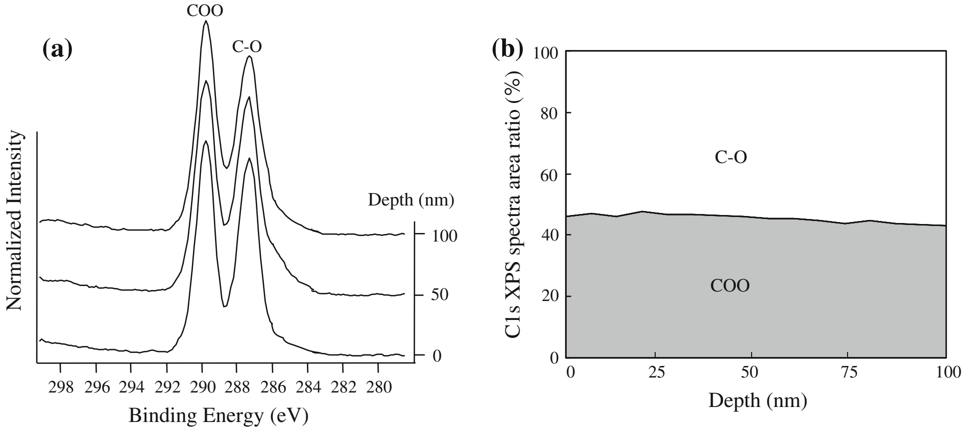

Fig. 6 a C1s XPS spectra of PGA, which were obtained before sputtering and after 50 and 100 nm sputtering. **b** XPS depth profile of PGA obtained using $C_{60}{}^{+}$ ion sputtering. The depth profile of C–O, COO bonds were obtained by analyzing C1s XPS spectra of every 1-min sputtering. The sputtering depth means reduced value of PVA (10 nm min^{-1})

Table 3 Change of the functional group content before and after C_{60}^{+} ion sputtering in various aliphatic polymers

	Abbreviation	Chemical constitution	Functional group	C1s XPS spectra area ratio (%)		Difference (%)
				Before sputtering	After sputtering[a]	
Aliphatic polymers	PGA	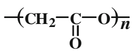 $\left(CH_2-\underset{\underset{O}{\|}}{C}-O\right)_n$	C–O	54	56	+2
			COO	46	44	−2
	PLA	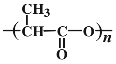 $\left(\underset{}{\overset{\overset{CH_3}{\mid}}{C}H}-\underset{\underset{O}{\|}}{C}-O\right)_n$	C–C	39	44	+5
			C–O	29	26	−3
			COO	32	30	−2
	PCL	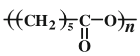 $\left((CH_2)_5-\underset{\underset{O}{\|}}{C}-O\right)_n$	C–C	61	63	+2
			C–O	25	25	+0
			COO	14	12	−2
	PBS	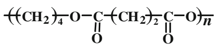 $\left((CH_2)_4-O-\underset{\underset{O}{\|}}{C}-(CH_2)_2-\underset{\underset{O}{\|}}{C}-O\right)_n$	C–C	51	47	−4
			C–O	29	32	+3
			COO	20	21	+1
	PAA	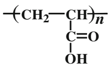 $\left(CH_2-\underset{\underset{\underset{OH}{\mid}}{\underset{C=O}{\mid}}}{C}H\right)_n$	C–C	70	80	+10
			COO	30	20	−10
	PMMA	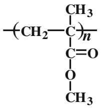 $\left(CH_2-\overset{\overset{CH_3}{\mid}}{\underset{\underset{\underset{\underset{CH_3}{\mid}}{\underset{O}{\mid}}}{\underset{C=O}{\mid}}}{C}}\right)_n$	C–C	56	61	+5
			C–O	26	23	−3
			COO	18	16	−2
	POM	$\left(CH_2-O\right)_n\left(CH_2CH_2-O\right)_m$	C–C	22	21	−1
			C–O	7	20	+13
			O–C–O	71	59	−12
	PVA	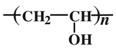 $\left(CH_2-\underset{\underset{OH}{\mid}}{C}H\right)_n$	C–C	44	43	−1
			C–O	56	51	−5
			C=O[b]	0	6	+6
	EVOH	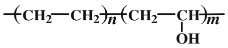 $\left(CH_2-CH_2\right)_n\left(CH_2-\underset{\underset{OH}{\mid}}{C}H\right)_m$	C–C	72	71	−1
			C–O	28	26	−2
			C=O[b]	0	3	+3
	PEG	$\left(CH_2-CH_2-O\right)_n$	C–C	0	10	+10
			C–O	100	90	−10
	PVC	$\left(CHCl-CH_2\right)_n$	C–C	54	71	+17
			C–Cl	46	29	−17
	PVDC	$\left(CCl_2-CH_2\right)_n$	C–C	71	87	+16
			$C–Cl_2$	29	13	−16
	PA	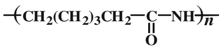 $\left(CH_2(CH_2)_3CH_2-\underset{\underset{O}{\|}}{C}-NH\right)_n$	C–C	68	70	+2
			C–N	17	15	−2
			O=C–N	15	15	+0

Table 3 continued

Abbreviation	Chemical constitution	Functional group	C1s XPS spectra area ratio (%)		Difference (%)
			Before sputtering	After sputtering[a]	
PAN	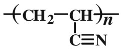 $-\!\!\left(CH_2-\underset{C\equiv N}{CH}\right)_{\!n}\!-$	C–C	54	59	+5
		C≡N	46	41	−5

[a] The sputtering depth means reduced value of PVA (10 nm min^{-1})

[b] Functional group newly detected after sputtering

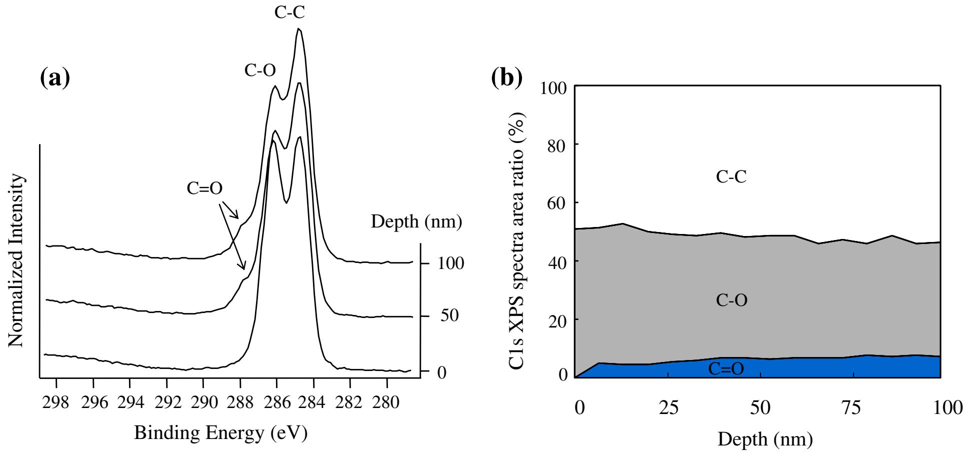

Fig. 7 **a** C1s XPS spectra of PVA, which were obtained before sputtering and after 50 and 100 nm sputtering. **b** XPS depth profile of PVA obtained using $C_{60}{}^{+}$ ion sputtering. The depth profile of C–C, C–O, and C=O bonds were obtained by analyzing C1s XPS spectra of every 1-min sputtering. The sputtering depth means reduced value of PVA (10 nm min^{-1})

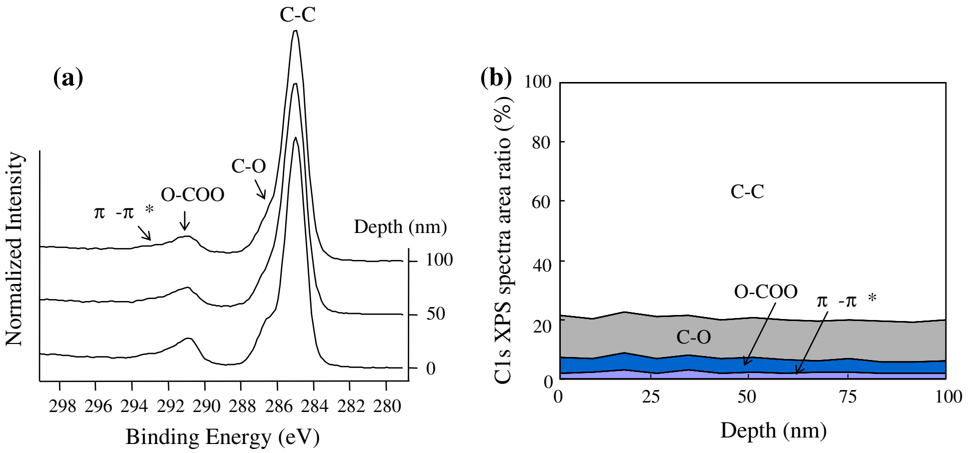

Fig. 8 **a** C1s XPS spectra of PC, which were obtained before sputtering and after 50 and 100 nm sputtering. **b** XPS depth profile of PC obtained using $C_{60}{}^{+}$ ion sputtering. The depth profile of C–C, C–O, O–COO bonds, and π–π* were obtained by analyzing C1s XPS spectra of every 1-min sputtering. The sputtering depth means reduced value of PET (5 nm min^{-1})

100 nm. In all the cases of PET, PBT, PEN, PEEK, PAI, PBI, PU, PSF, and PES, the ratio of change of the functional group derived from each chemical structure was less than ±8%. From these results, it was concluded that the $C_{60}{}^{+}$ ion sputtering is practically applicable to the depth profile XPS analysis of aromatic polymers.

Table 4 Change of the functional group content before and after C_{60}^{+} ion sputtering in various aromatic polymers

	Abbreviation	Chemical constitution	Functional group	C1s XPS spectra area ratio (%)		Difference (%)
				Before sputtering	After sputtering[a]	
Aromatic polymers	PC	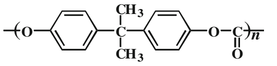	C–C	76	78	+2
			C–O	14	13	−1
			O–COO	5	4	−1
			π–π*	5	5	+0
	PET	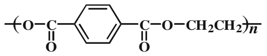	C–C	57	63	+6
			C–O	19	16	−3
			COO	20	17	−3
			π–π*	4	4	+0
	PBT	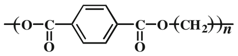	C–C	66	68	+2
			C–O	20	18	−2
			COO	12	12	+0
			π–π*	2	2	+0
	PEN	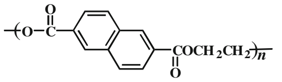	C–C	67	71	+4
			C–O	16	14	−2
			COO	12	10	−2
			π–π*	5	5	+0
	PEEK	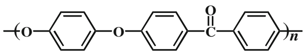	C–C	59	63	+4
			C–O	33	29	−4
			C=O	4	4	+0
			π–π*	4	4	+0
	PAI	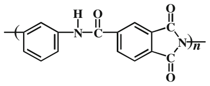	C–C	85	87	+2
			O=C–N	8	7	−1
			π–π*	7	6	−1
	PBI	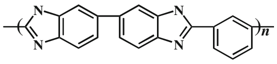	C–C	68	68	+0
			C–N, N–C=N	20	20	+0
			π–π*	12	12	+0
	PU	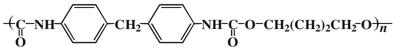	C–C	53	54	+1
			C–O, C–N	42	41	−1
			N=COO	4	4	+0
			π–π*	1	1	+0
	PSF	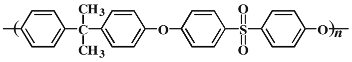	C–C, C–S	81	83	+2
			C–O	14	12	−2
			π–π*	5	5	+0
	PES	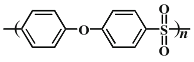	C–C, C–S	80	81	+1
			C–O	15	14	−1
			π–π*	5	5	+0

[a] The sputtering depth means reduced value of PET (5 nm min^{-1})

Fluorine containing polymers

Figure 9 shows the (a) C1s XPS spectra and (b) XPS depth profile of PTFE. In (a) C1s XPS spectra, the new peaks can be identified as the C–CF_2, CF, and CF_3 bonds in addition to the original CF_2 bond. This result is the same as the case of Ar^{+} ion sputtering shown in Fig. 4. In (b) XPS depth profile, the ratios of the C–CF_2 bond, the CF bond, and the

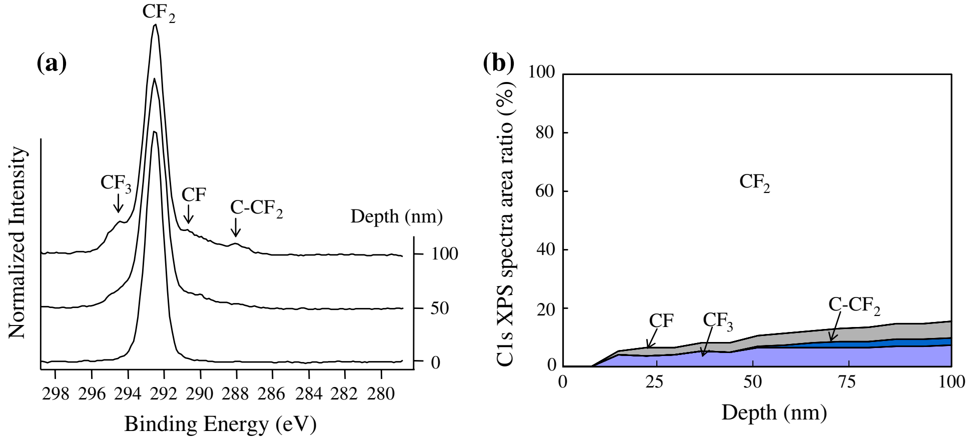

Fig. 9 **a** C1s XPS spectra of PTFE, which were obtained before sputtering and after 50 and 100 nm sputtering. **b** XPS depth profile of PTFE obtained using $C_{60}{}^+$ ion sputtering. The depth profile of CF$_2$, CF, C–CF$_2$, and CF$_3$ bonds were obtained by analyzing C1s XPS spectra of every 1-min sputtering. The sputtering depth means reduced value of ETFE (20 nm min^{-1})

Table 5 Change of the functional group content before and after $C_{60}{}^+$ ion sputtering in various fluorine containing polymers

	Abbreviation	Chemical constitution	Functional group	C1s XPS spectra area ratio (%)		Difference (%)
				Before sputtering	After sputtering[a]	
Fluorine containing polymers	PTFE	$-\!(CF_2-CF_2)_n\!-$	C–CF$_2$[b]	0	2	+2
			CF[b]	0	5	+5
			CF$_2$	100	87	−13
			CF$_3$[b]	0	6	+6
	PVDF	$-\!(CF_2-CH_2)_n\!-$	C–CF$_2$	52	53	+1
			CF[b]	0	12	+12
			CF$_2$	48	33	−15
			CF$_3$[b]	0	2	+2
	ETFE	$-\!(CF_2-CF_2)_n\!-\!(CH_2-CH_2)_m\!-$	C–C	36	37	+1
			CF[b]	0	15	+15
			CF$_2$	64	44	−20
			CF$_3$[b]	0	4	+4
	PFA	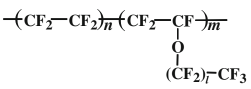 $-\!(CF_2-CF_2)_n\!-\!(CF_2-\underset{\underset{(CF_2)_l-CF_3}{\mid}}{\underset{O}{\underset{\mid}{CF}}})_m\!-$	C–CF$_2$[b]	0	3	+3
			CF	1	6	+5
			CF$_2$	97	84	−13
			CF$_3$	2	7	+5

[a] The sputtering depth means reduced value of ETFE (20 nm min^{-1})

[b] Functional group newly detected after sputtering

CF$_3$ bond increased gradually as sputtering was repeated. However, while the decrease ratio of the CF$_2$ bond derived from the PTFE structure after the 100-nm sputtering was 40% in the case of Ar$^+$ ion, this ratio was 13% in the case of $C_{60}{}^+$ ion. Table 5 shows the ratio of change of each functional groups of other fluorine containing polymers through the $C_{60}{}^+$ ion sputtering at a depth of 100 nm. In these polymers, the formation of new bonds was observed by $C_{60}{}^+$ ion sputtering, and the chemical structures were changed. Here, the decrease ratio of the CF$_2$ bond derived from the PVDF and ETFE structures was more than 40% for Ar$^+$ ion sputtering, and less than 20% for $C_{60}{}^+$ ion sputtering. This indicates that the damage of chemical structure reduced considerably by using $C_{60}{}^+$ ion. From these results, we can conclude that the change of chemical structures of fluorine containing polymers by $C_{60}{}^+$ ion is much lower than those for Ar^+ ion sputtering. In addition, it was considered that fluorine containing polymers have a tendency to undergo bond dissociation, compositional mixing, and recombination, compared with other polymers.

Natural polymers

Figure 10 shows the (a) C1s XPS spectra and (b) XPS depth profile of TAC. In the case of Ar^+ ion shown in Fig. 5, the ratios of the C–O, O–C–O, and COO bonds derived from the TAC structure decreased gradually as sputtering was repeated. However, in the case of $C_{60}{}^+$ ion sputtering, the spectra form of after sputtering (50 and 100 nm) did not change through sputtering. In (b) XPS depth profile, the ratio of change of oxygen containing functional groups after the 100-nm sputtering was less than ±5%. On the other hand, Table 6 shows the results for CEL having a similar structure to TAC. New peaks that can be identified as the C–C bond and the COO bond were observed after sputtering. The appearance of the C–C bond indicates the carbonization of the surface due to $C_{60}{}^+$ ion sputtering. In addition, we can conclude that the hydroxyl groups in the CEL structure oxidized, because the ratio of the O–C–O bond was almost the same and the ratio of the C–O bond decreased by $C_{60}{}^+$ ion sputtering. The behaviors of natural polymers are similar to those of aliphatic polymers.

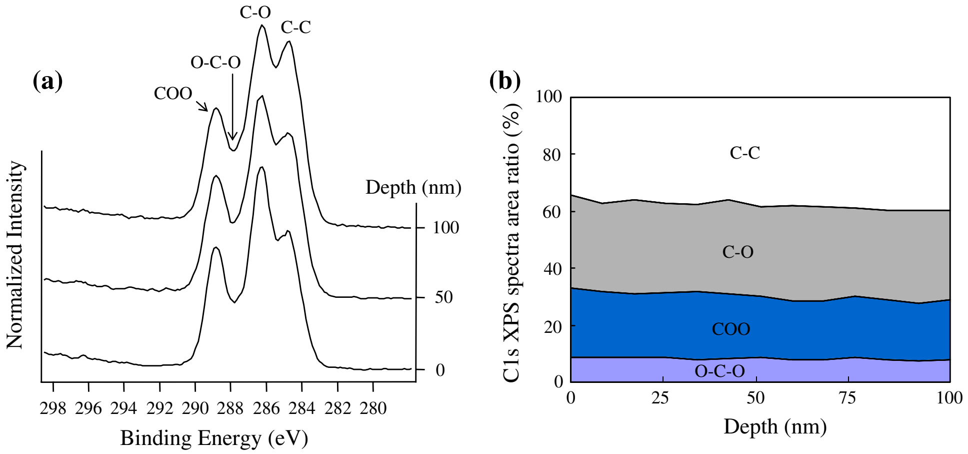

Fig. 10 **a** C1s XPS spectra of TAC, which were obtained before sputtering and after 50 and 100 nm sputtering. **b** XPS depth profile of TAC obtained using $C_{60}{}^+$ion sputtering. The depth profile of C–C, C–O, O–C–O, and COO bonds were obtained by analyzing C1s XPS spectra of every 1-min sputtering. The sputtering depth means reduced value of TAC (20 nm min^{-1})

Table 6 Change of the functional group content before and after $C_{60}{}^+$ ion sputtering in natural polymers

	Code address	Chemical constitution	Functional group	C1s XPS spectra area ratio (%)		Difference (%)
				Before sputtering	After sputtering[a]	
Natural polymers	TAC	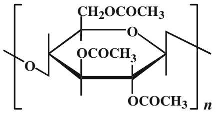	C–C	34	40	+6
			C–O	33	31	−2
			O–C–O	9	8	−1
			COO	24	21	−3
	CEL	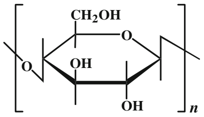	C–C[b]	0	13	+13
			C–O	79	64	−15
			O–C–O	21	19	−2
			COO[b]	0	4	+4

[a] The sputtering depth means reduced value of TAC (20 nm min^{-1})

[b] Functional group newly detected after sputtering

Conclusions

In this research, the depth profile XPS analysis of aliphatic polymers, aromatic polymers, fluorine containing polymers, and natural polymers were conducted with the sputtering source being C_{60}^{+} ion, and the degree of damage was evaluated in detail comparing with the results by conventional Ar^{+} ion sputtering. As a result, it was found that Ar^{+} ion sputtering induces significant carbonization in all polymers. Meanwhile, it turned out that C_{60}^{+} ion sputtering causes little damage to most polymers. However, the damage by C_{60}^{+} ion sputtering has a tendency to increase slightly in the case of the non-aromatic polymers containing halogen, hydroxyl, carboxyl, and ether groups.

References

1. Bachman BJ, Vasile MJ (1989) J Vac Sci Technol A 7:2709
2. Briggs D (1998) Surface analysis of polymers by XPS and static SIMS. Cambridge University Press, Cambridge
3. Castner DG (2003) Nature 422:122
4. Wong SCC, Hill R, Blenkinsopp P, Lockyer NP, Weibel DE, Vickerman JC (2003) Appl Surf Sci 203:219
5. Cheng J, Wucher A, Winograd N (2006) J Phys Chem B 110:8329
6. Touboul D, Kollmer F, Niehuis E, Brunelle A, Laprevote O (2005) J Am Soc Mass Spectrom 1608:16
7. Weibel DE, Lockyer N, Blenkinsopp P, Hill R, Vickerman JC (2003) Anal Chem 75:1754
8. Weibel DE, Lockyer N, Vickerman JC (2004) Appl Surf Sci 146:231
9. Sun S, Szakal C, Smiley E, Postawa Z, Wucher A, Winograd N (2004) Appl Surf Sci 231–232:64
10. Sun S, Szakal C, Roll T, Mazarov P, Wucher A, Winograd N (2004) Surf Interface Anal 36:1367
11. Kollmer F (2004) Appl Surf Sci 231–232:153
12. Winograd N (2005) Anal Chem 77:143A
13. Hinder SJ, Lowe C, Watts JF (2007) Surf Interface Anal 39:467
14. Postawa Z, Czerwinski B, Szewczyk M, Smiley EJ, Winograd N, Garrison BJ (2003) Anal Chem 75:4402
15. Postawa Z, Czerwinski B, Szewczyk M, Smiley EJ, Winograd N, Garriso BJ (2004) J Phys Chem B 108:7831
16. Gillen G, Batteas J, Michaels CA, Chi P, Small J, Windsor E, Fahey A, Verkouteren J, Kim KJ (2006) Appl Surf Sci 252:6521
17. Miyayama T, Inoue R, Sanada N (2007) Hyoumen Kagaku 28:504
18. Sanada N, Yamamoto A, Oiwa R, Ohashi Y (2004) Surf Interface Anal 36:280
19. Yamamoto Y, Shirota N, Yamamoto K (2007) Hyoumen Kagaku 28:348
20. Sakai D, Sanada N, Hammond JS, Iwai H (2005) J Surf Anal 12:97
21. Beamson G, Briggs D (1992) High resolution XPS of organic polymers. The scienta ESCA300 database. Wiley, Chichester
22. Suzuki M, Mogi K, Ando H (1999) J Surf Anal 5:188